Systemic knockout of Tspo in mice does not affect retinal morphology, function and susceptibility to degeneration.

Klee, Katrin ; Storti, Federica ; Barben, Maya ; Samardzija, Marijana ; Langmann, Thomas ; Dunaief, Joshua ; Grimm, Christian

Abstract: Translocator protein (18 kDa) (TSPO) is a mitochondrial protein expressed by reactive microglia and astrocytes at the site of neuronal injury. Although TSPO function has not been fully determined, synthetic TSPO ligands have beneficial effects on different pathologies of the central nervous system, including the retina. Here, we studied the pattern of Tspo expression in the aging human retina and in two mouse models of retinal degeneration. Using a newly generated Tspo-KO mouse, we investigated the impact of the lack of TSPO on retinal morphology, function and susceptibility to degeneration. We show that TSPO was expressed in both human and mouse retina and retinal pigment epithelium (RPE). Tspo was induced in the mouse retina upon degeneration, but constitutively expressed in the RPE. Similarly, TSPO expression levels in healthy human retina and RPE were not differentially regulated during aging. Tspo-KO mice had normal retinal morphology and function up to 48 weeks of age. Photoreceptor loss caused either by exposure to excessive light levels or by a mutation in the phosphodiesterase 6b gene was not affected by the absence of Tspo. The reactivity states of retinal mononuclear phagocytes following light-damage were comparable in Tspo-KO and control mice. Our data suggest that lack of endogenous TSPO does not directly influence the magnitude of photoreceptor degeneration or microglia activation in these two models of retinal degeneration. We therefore hypothesize that the interaction of TSPO with its ligands may be required to modulate disease progression.

DOI: https://doi.org/10.1016/j.exer.2019.107816

Experimental Eye Research 188 (2019) 107816

Contents lists available at ScienceDirect

Experimental Eye Research

journal homepage: www.elsevier.com/locate/yexer

Systemic knockout of *Tspo* in mice does not affect retinal morphology, function and susceptibility to degeneration

Katrin Klee[a,b], Federica Storti[a], Maya Barben[a], Marijana Samardzija[a], Thomas Langmann[c,d], Joshua Dunaief[e], Christian Grimm[a,b,f,*]

[a] Lab for Retinal Cell Biology, Department of Ophthalmology, University of Zurich, Schlieren, Switzerland
[b] Center for Integrative Human Physiology (ZIHP), University of Zurich, Zurich, Switzerland
[c] Laboratory for Experimental Immunology of the Eye, Department of Ophthalmology, University of Cologne, Faculty of Medicine and University Hospital Cologne, Cologne, Germany
[d] Center for Molecular Medicine Cologne (CMMC), Cologne, Germany
[e] Department of Ophthalmology, Scheie Eye Institute, University of Pennsylvania, Philadelphia, PA, USA
[f] Neuroscience Center, University of Zurich, Zurich, Switzerland

ARTICLE INFO

Keywords:
Retina
TSPO
Microglia
Retinal degeneration
RPE

ABSTRACT

Translocator protein (18 kDa) (TSPO) is a mitochondrial protein expressed by reactive microglia and astrocytes at the site of neuronal injury. Although TSPO function has not been fully determined, synthetic TSPO ligands have beneficial effects on different pathologies of the central nervous system, including the retina. Here, we studied the pattern of *Tspo* expression in the aging human retina and in two mouse models of retinal degeneration. Using a newly generated *Tspo*-KO mouse, we investigated the impact of the lack of TSPO on retinal morphology, function and susceptibility to degeneration. We show that *TSPO* was expressed in both human and mouse retina and retinal pigment epithelium (RPE). *Tspo* was induced in the mouse retina upon degeneration, but constitutively expressed in the RPE. Similarly, *TSPO* expression levels in healthy human retina and RPE were not differentially regulated during aging. *Tspo*-KO mice had normal retinal morphology and function up to 48 weeks of age. Photoreceptor loss caused either by exposure to excessive light levels or by a mutation in the phosphodiesterase 6b gene was not affected by the absence of *Tspo*. The reactivity states of retinal mononuclear phagocytes following light-damage were comparable in *Tspo*-KO and control mice. Our data suggest that lack of endogenous TSPO does not directly influence the magnitude of photoreceptor degeneration or microglia activation in these two models of retinal degeneration. We therefore hypothesize that the interaction of TSPO with its ligands may be required to modulate disease progression.

1. Introduction

Translocator protein (18 kDa) (TSPO) was identified in 1977 (Braestrup et al., 1977) and initially named peripheral benzodiazepine receptor. TSPO is a 169-amino acid protein located in the outer mitochondrial membrane (Anholt et al., 1985) (reviewed in(Rupprecht et al., 2010)) and encoded by a nuclear gene consisting of four exons, with exon two containing the START-codon (Sileikyte et al., 2014). TSPO forms a channel with five α-helical transmembrane domains and contains a cholesterol-recognition amino acid consensus (CRAC) sequence at its C-terminal end that folds toward the lipid membrane (Jaremko et al., 2014). TSPO has been connected to the mitochondrial transition pore regulation (Chelli et al., 2001) (Azarashvili et al., 2015), steroid synthesis (reviewed in (Rupprecht et al., 2010; Selvaraj et al., 2015)), Ca^{2+} homeostasis (Gatliff et al., 2017), reactive oxygen species production (Gatliff et al., 2014) and energy metabolism (Liu et al., 2017; Tu et al., 2016). However, none of these functions has been broadly confirmed and the molecular and physiological role of TSPO remains elusive.

TSPO was first identified as a peripheral binding site for benzodiazepines, such as diazepam. Since benzodiazepines are used to treat psychiatric disorders, TSPO ligands were investigated as possible therapeutics. Indeed, TSPO ligands exerted beneficial outcomes for anxiety disorders in animal models and human patients (reviewed in (Nothdurfter et al., 2012; Rupprecht et al., 2010; Rupprecht et al., 2009). It was suggested that this effect may be related to the ability of the ligands to increase levels of (neuro)steroids, such as allopregnanolone, and therefore modulate activity of GABAA (Bitran et al., 2000;

* Corresponding author. Lab for Retinal Cell Biology Department Ophthalmology, University of Zürich, Wagistrasse 14, CH 8952, Schlieren, Switzerland.
E-mail address: cgrimm@opht.uzh.ch (C. Grimm).

https://doi.org/10.1016/j.exer.2019.107816
Received 25 June 2019; Received in revised form 19 September 2019; Accepted 24 September 2019
Available online 25 September 2019

Table 1
Genotyping primers.

Gene	Forward 5′-3′	Reverse 5′-3′
Tspo flox/flox (Šileikytė et al., 2014)	GGATTACCACACCCAACCAG	TAGGAGTGCAAAGCCAGTCA
Tspo excision	GCTGGAATGACAGGTGGAT	CCTCTGTTCTCAGCTTCAGT
$Tspo_{168Pro}$	CCACCGTGCTCAACTACTA	GCCCAATGGTCATAAAAG
$Rpe65_{450Leu}$ (Grimm et al., 2004)	CACTGTGGTCTCTGCTATCTTC	GGTGCAGTTCCACTTCAGTT
Tyr c/c (Alexeev and Yoon, 1998)	AAGAATGCTGCCCACCATG	GACATAGACTGAGCTGATAGTATGTT
BEST1-Cre (Iacovelli et al., 2011)	ATGCCCAAGAAGAAGAGGAAGGTGTCC	GCCCAATGGTCATAAAAG

Nothdurfter et al., 2012; Rupprecht et al., 2009). High levels of TSPO in steroidogenic tissues such as gonads, adrenals and brain (Papadopoulos et al., 2006), its localization in the outer mitochondrial membrane (Anholt et al., 1985), its channel-like structure and the presence of a CRAC on its cytosolic terminal (Jaremko et al., 2014) made TSPO an appealing candidate for being involved in cholesterol trafficking. Thus, TSPO was proposed to transport cholesterol from the cytosol into the mitochondrial matrix, the rate limiting step in steroidogenesis (Papadopoulos et al., 2006). However, recent studies have failed to detect any deficit in steroid synthesis following genetic ablation of *Tspo*, reopening the debate about the role of *Tspo* in steroidogenesis (Morohaku et al., 2014; Sileikyte et al., 2014; Tu et al., 2014, 2016). Interestingly, transcriptomic analysis of adrenal glands from *Tspo-KO* mice revealed no effect on steroidogenic pathways but detected differential regulation of genes involved in the immune response (Tu et al., 2014). Indeed, it is generally accepted that TSPO is regulated in various immune cell populations. Following brain injury for example, TSPO levels increase in primary and secondary injury sites due to activation of microglia (reviewed in (Bennett et al., 2016)) and astrocytes (Cosenza-Nashat et al., 2009; Guilarte, 2019). Its regulation in brain microglia and astrocytes during pathologies and its specific interaction with several radioligands makes TSPO an attractive tool to diagnose and follow neuroinflammation by positron-emission tomography (PET; reviewed in (Best et al., 2019)).

Furthermore, application of TSPO ligands showed positive effects in mouse models for neuropathies, such as peripheral nerve lesions, Parkinson's disease, Alzheimer disease and multiple sclerosis (Gong et al., 2019; Guilarte, 2019; Leva et al., 2017) reviewed in (Best et al., 2019). Similarly, recent data also support a neuroprotective potential of systemically applied TSPO ligands for retinal structures (Leva et al., 2017; Scholz et al., 2015). Scholz et al. demonstrated that XBD173, a synthetic TSPO ligand, dampened microglia activation and preserved the retinal structure in Balb/c mice following exposure to toxic levels of light (Scholz et al., 2015).

In view of the increasing diagnostic and therapeutic relevance of TSPO ligands for brain and retinal pathologies, it is important to better characterize TSPO function and regulation. Although TSPO is expressed in the mouse neural retina and retinal pigment epithelium (RPE) and TSPO ligands may influence retinal homeostasis in pathogenic situations (Karlstetter et al., 2014; Scholz et al., 2015), not much is known about its dynamics and potential function in ocular tissues. Thus, we studied TSPO expression in different mouse models of retinal degeneration and in human retinas collected from post-mortem donors. We also generated a $Tspo^{-/-}$ mouse (*Tspo-KO*), followed its retinal development and function, and analysed the susceptibility of its retina to stress-induced degeneration.

2. Material and methods

2.1. Mice and generation of Tspo knockouts

Mouse colonies were maintained at the Laboratory Animal Service Center (LASC) of the University of Zurich under a cycle of 14 h light and 10 h darkness with free access to food and water. Mice were euthanized by suffocation with CO_2 followed by cervical dislocation. All experiments were approved by the veterinary authorities of Canton Zurich, Switzerland and adhered to the ARVO Statement for the Use of Animals in Ophthalmic and Vision Research.

Tspo-KO mice were generated on a mixed background by crossing $Tspo^{flox/flox}$ (Sileikyte et al., 2014) mice with *BEST1-Cre* mice (Iacovelli et al., 2011). To introduce the $Rpe65_{450Leu}$ variant that increases light-damage susceptibility (Wenzel et al., 2001), $Tspo^{flox/flox}$; *BEST1*-Cre mice were backcrossed to Balb/c mice for one generation, followed by the intercross of F1 pups. To obtain homogeneous fur pigmentation within our mouse colony, we selected mice homozygous for tyrosinase^{Cys95} (Alexeev and Yoon, 1998). A naturally occurring single nucleotide polymorphism (e.g. in 129/S6 mice) in *Tspo* causes the exchange of proline with alanine at amino acid position 168. Since this renders TSPO not detectable with our anti-TSPO antibody (CAT: ab109497, AbCam, Cambridge, UK), mice homozygous for the $Tspo_{168Pro}$ variant were selected for further breeding. *BEST1-Cre* is occasionally active in germ line cells resulting in offspring carrying monoallelic excision of the floxed gene (Iacovelli et al., 2011). Mice bearing a monoallelic excision of *Tspo* were intercrossed to generate biallelic whole-body *Tspo-KOs*. $Tspo^{flox/flox}$ mice were used as controls (CTRL).

Tspo-KO mice were also crossed with *rd10* mice that carry a mutation in phosphodiesterase 6b ($Pd6b^{rd10}$) leading to photoreceptor loss (reviewed in (Chang et al., 2002)). Briefly, *Tspo-KO* mice were bred with $Pd6b^{rd10}$ mice to generate $Tspo^{-/-}$;*rd10/rd10* (*Tspo-KO;rd10*) mice in the second generation. *rd10/rd10* (*rd10*) were used as controls. Mice were genotyped by conventional PCR on genomic DNA isolated from ear biopsies using specific primer pairs listed in Table 1.

2.2. Light damage

Eyes of dark-adapted mice were dilated under dim-red light with 1% cyclogyl (Alcon Pharmaceutical, Cham, Switzerland) and 5% phenylephrine (Ciba Vision, Niederwangen, Switzerland). Mice were then single caged in aluminium-coated cages and exposed to 10′000 lux of white light for 2 h. Following light exposure, mice were returned to their normal housing cages and kept in darkness overnight before returning them to a 12 h:12 h light-dark cycle. Tissues were collected at 12 h, and at 4 and 14 days post-exposure. Dark control mice (DC) were treated in parallel but kept in darkness.

2.3. Electroretinography (ERG)

Mice were dark-adapted over night. Prior to ERG recording, pupils were dilated as described above. Mice were anesthetized by a subcutaneous injection of a mixture of Ketamine (85 mg/kg, Parke-Davis, Berlin, Germany) and Rompun (Xylazine, 4 mg/kg, Bayer AG, Leverkusen, Germany) and placed on a heated pad. Golden ring electrodes were placed onto each cornea. Mice were exposed to light flashes ranging from −50 dB (0.000025 cd*s/m^2) to 15 dB (79 cd*s/m^2) for scotopic and from −10 dB (25 cd*s/m^2) to 25 dB (790 cd*s/m^2) for photopic ERG. Mice were light-adapted for 5 min prior to photopic ERG. Light-evoked retinal responses were recorded with an LKC UTAS Bigshot unit (LKC Technologies, Inc. Gaithersburg, MD, USA). For each light intensity, 10 recordings were averaged.

2.4. Optical coherence tomography (OCT)

Dilation of pupils and anaesthesia were performed as described above. A drop of 2% Methocel (OmniVision AG, Neuhausen, Switzerland) was applied to each eye to keep the cornea moist. Mice were placed on a heated holder and fundus images and OCT scans were acquired using the Micron IV system (Phoenix Research Labs, Pleasanton, CA, USA).

2.5. Tissue dissection

Eyes of euthanized mice were held in place using a pair of forceps. The eyeballs were opened by slitting the cornea using a sharp scalpel. Lens and vitreous were removed through this slit, the neural retina isolated and quickly frozen in liquid nitrogen. The remaining eyecup (EC, representative for RPE/choroid) was cut from the eye socket using scissors and frozen in liquid nitrogen.

2.6. Retinal flat mounts

Preparation of retinal flat mounts was as described recently (Caprara et al., 2011). Briefly, left and right eyes were enucleated and fixed for 10 min in 4% PFA (in 0.1 M phosphate buffer). Thereafter, the cornea was punched and eyes were post-fixed for additional 20 min in 4% PFA. Eyeballs were opened, cut into a cloverleaf shape and flattened with brushes. The lens was carefully removed and the retina was gently pulled away from the eyecup. Isolated retinas were post-fixed for 1 h in 4% PFA and incubated for 1 h in blocking solution (3% normal goat serum (Sigma-Aldrich, St. Louis, MO, USA), 0.3% Triton X-100 (Sigma-Aldrich, Buchs SG, Switzerland)). Flat mounts were stained following the standard immunofluorescence protocol (see 2.9 Immunofluorescence) and mounted on glass slides.

2.7. Human retina and RPE samples

Collection of eye bulbs from post-mortem donors at the University Hospital of Zurich was approved by the ethics committee of Canton Zurich, Switzerland (BASEC-Nr: PB_2017-00550), and adhered to the tenets of the Declaration of Helsinki. Donor age ranged from 17 to 90 years. Only eyes from donors without diagnosed eye disease were included in the study. Age, gender and known diseases of donors are listed in Table 2. After removal of the cornea, eyeballs were immerged in PBS and cut into a clover-leaf structure. Lens and vitreous were carefully removed and nasal mid-peripheral and central retina dissected. Retina and RPE were isolated separately, snap frozen and stored in liquid nitrogen until use. RNA was isolated using the RNeasy kit (Qiagen, Hilden, Germany) following the manufacturer's instruction. cDNA synthesis was as described below.

Table 2
Details about human donors.

Human eye	Age	Gender	Known disease
6	57	M	–
7	77	M	–
8	90	M	–
9	76	M	Adenocarcinoma
10	65	M	Diabetes Type 2
11	58	M	Colitis ulcerosa
12	64	M	–
13	80	F	Coronary disease
14	58	F	Depression
16	74	M	–
17	78	M	Coronary disease
18	83	F	–
19	17	M	–
21	83	F	Hypertension
22	46	M	Leukemia
23	82	M	–
24	83	F	Epilepsy
25	31	M	–
26	53	M	Hypertension
27	34	F	Alcohol addition
28	59	F	Diabetes Type

2.8. Western blotting

Proteins were isolated from whole neural retinas, ECs or small fragments of kidney and liver. Tissues were homogenised in 200 µl of Tris-HCL (100 mM, pH 8.0) by sonication and centrifuged for 3 min at 1′000 rcf. Protein concentration was determined in the supernatant using the Bradford assay reagent (BioRad, Cressier, Switzerland). 30 µg of proteins were loaded onto an SDS-PAGE, separated according to their size and transferred to a nitrocellulose membrane. The membrane was blocked using 5% non-fat milk as blocking agent (BioRad, Cressier, Switzerland) and incubated over night at 4 °C with anti-TSPO (1:2′500, ab109497, AbCam, Cambridge, UK) and anti-ACTB (1:1′000, A5441, Sigma-Aldrich, Buchs SG, Switzerland) antibodies diluted in 5% blocking milk. Thereafter, membranes were incubated with the appropriate HRP-conjugated secondary antibody (anti-mouse, 1:10′000, sc-2031, Santa Cruz, Nunningen, Switzerland; anti-rabbit 1:10′000, P-5282, Sigma-Aldrich, Buchs SG, Switzerland). ECL-chemoluminescence (PerkinElmer, Waltham, MA, USA) was visualized using an X-Ray film.

2.9. Immunofluorescence

Following euthanasia, the right eye was marked nasally and enucleated. Eyes were fixed in 4% PFA (in 0.1 M phosphate buffer) for 2 h. Then the cornea was cut and eyes were returned to PFA for over night incubation at 4 °C. After removal of the lens, eyes were post-fixed for 2 h in 4% PFA at 4 °C, immerged in 30% sucrose for 2 h and embedded in aluminium molds filled with tissue freezing medium (O.C.T., Leica Biosystems Nussloch GmbH, Nussloch, Germany). Blocks were stored at −80 °C until sectioning. 12 µm thick cryosections containing the optic nerve head were blocked for 1 h at room temperature in blocking solution (3% normal goat serum (Sigma-Aldrich, St. Louis, MO, USA), 0.3% Triton X-100 (Sigma-Aldrich, Buchs SG, Switzerland)). Then, cryosections were incubated with the primary antibody (anti-TSPO, 1:500, ab109497, AbCam, Cambridge, UK; anti-IBA-1, 1:500, 019–19741, Wako Chemicals GmbH, Neuss, Germany) over night at 4 °C. Following three wash steps with phosphate-buffered saline, cryosections were incubated with secondary antibodies (Cy3-labelled anti-rabbit, 111-165-003, Jackson ImmunoResearch Laboratories, Westgrove, PA, USA) for 1 h at room temperature and nuclei were counterstained with DAPI (4′,6-Diamidine-2′-phenylindole dihydrochloride, Roche, Basel, Switzerland). Fluorescent signals were analysed by fluorescence microscopy (Axioplan 2, Zeiss, Feldbach, Switzerland).

2.10. Morphology

Following euthanasia, the cornea of the left eye was marked dorsally. Eyes were enucleated, fixed over night at 4 °C in 2.5% glutaraldehyde/0.1 M cacodylate buffer and cut through the optic nerve head into a dorsal and ventral part. Both dorsal and ventral retina were washed in cacodylate buffer (0.1 M, pH 7.2), fixed for 1 h at room temperature in 1% osmium tetroxide (in cacodylate buffer). Following dehydration, retinas were embedded in Epon, cut into 0.5 µm thick sections and counterstained with toluidine blue. Ventral retinas were analysed by light microscopy with an Axioplan 2 microscope (Zeiss).

2.11. Nuclei and quantification of IBA1-positive microglia cells

Images of retinal morphologies were merged to generate panoramas

using Adobe Photoshop CS6 (Adobe Systems Inc., San Jose, CA, USA). Nuclei counts were performed by placing 75 μm × 37.5 μm squares (2′812.5 μm^2) on the ONL at 200, 400, 800, 1′200 and 1′600 μm distance on either side of the optic nerve head. The short edge of the square was placed parallel to the RPE. Nuclei in this square were manually counted using ImageJ (Schneider et al., 2012).

IBA1-positive cells were quantified on retinal flat mounts using ImageJ (Schneider et al., 2012). For each flat mount, a rectangular area of 450 μm^2 × 320 μm^2 was selected in each of the four arms of the cloverleaf-shaped retina in an equal distance from the optic nerve. IBA1-positive cells were counted in these areas discarding microglias/macrophages crossing the area border. The focus plane was on the GCL for dark control mice since resident microglia are found in this layer of non-stressed retinas. The focus plane was shifted to the ONL in light exposed retinas as IBA1-positive cells move toward the ONL upon photoreceptor damage.

2.12. RNA isolation, cDNA synthesis and real-time PCR

Retina and ECs were homogenised by passing the tissue 10 times through a 21G needle. EC homogenates were centrifuged for 3 min at 3′000 rcf to pellet the sclera and RNA purification was performed on the supernatant. Total RNA was isolated using the MN Nucleo Spin RNA isolation Kit (Macherey-Nagel, Oensingen, Switzerland). cDNA was synthetized using oligo-dT primers and M-MLV reverse transcriptase (Promega, Dübendorf, Switzerland). 10 ng of cDNA were used to determine relative transcript levels of specific genes by real-time PCR using an ABI QuantStudio3 device (Thermo Fisher Scientific, Waltham, MA, USA), the PowerUp SYBR Green master mix (Thermo Fisher Scientific) and specific primer pairs (Table 3). Transcript levels were normalized to *Actb* and relative expression calculated using the $\Delta\Delta C_t$ method using the Thermo Fisher Cloud software. LightCycler480 (Roche Diagnostics, Rotkreuz, Switzerland) with SybrGreen I master mix (Roche Diagnostics) was used to measure *Tspo* mRNA levels in the retina and eyecup of B6 and *rd10* mice (Fig. 2A). Normalization of transcript levels was performed with the LightCycler480 software (Roche Diagnostics, Rotkreuz, Switzerland).

3. Results

3.1. Tspo is highly expressed in the mouse RPE

We have recently shown that TSPO is expressed not only in the mouse retina but also in the RPE (Scholz et al., 2015; Storti et al., 2017). Using semi-quantitative real-time PCR we now estimated its relative expression levels in both tissues. Since a direct comparison of mRNA levels in different tissues is not possible by this method due to potentially different expression levels of the reference gene, we determined cycle threshold (Ct) values of *Tspo* and *Actb* in 10 ng cDNA from the mouse retina and eyecup (EC). Whereas mean Ct values of *Actb* were not different between ECs (Ct: 18.63) and retina (Ct: 19.26), Ct values of *Tspo* were significantly lower in the EC (Fig. 1A), suggesting several-fold higher expression levels of *Tspo* mRNA in EC. Immunofluorescence staining on mouse cryosections confirmed the high expression level of TSPO in the RPE whereas signals were weak in the retina and confined to the inner layers, probably coming from labelled blood vessels (Wang et al., 2014) and astrocytes (Cosenza-Nashat et al., 2009) cells (Fig. 1B).

3.2. Retinal degeneration upregulates Tspo in the retina but not EC

Despite the controversial results about TSPO function, there is a general consensus that expression of TSPO is upregulated in reactive microglia in the CNS including the retina (Karlstetter et al., 2014; Scholz et al., 2015) reviewed in (Bennett et al., 2016; Guilarte, 2019). To determine whether expression of *Tspo* is also regulated in ECs upon retinal degeneration, we measured *Tspo* transcript levels in retinas and ECs of two degenerative mouse models that are characterized by primary defects in rods (*rd10*; reviewed in(Chang et al., 2002)) or RPE cells ($RPE^{\Delta Abca1;Abcg1}$; (Storti et al., 2019);). Whereas retinas of *rd10* mice start to degenerate around post-natal day (PND) 15 (Samardzija et al., 2012), RPE-specific conditional *Abca1* and *Abcg1* double knockouts ($RPE^{\Delta Abca1;Abcg1}$ *BEST1*-Cre+) show strong retinal degeneration and RPE defects around 24 weeks of age (Storti et al., 2019). Both models had increased retinal expression levels of *Tspo* concomitantly with degeneration of the retina and microglia activation (Fig. 2A and B; upper panels). Expression of *Tspo* in the EC, however, was not induced by the degenerative processes in the retina and/or in the RPE (Fig. 2A and B; lower panels), suggesting that *Tspo* expression is regulated in the retina, but constitutive in the EC.

TSPO has been shown to be expressed in the human retina as well (Karlstetter et al., 2014; Storti et al., 2019), but to our knowledge its *in vivo* expression in the human RPE has not been described. We therefore determined *TSPO* mRNA levels in the peripheral and central retina and RPE of 21 human donor eyes that were not diagnosed with retinal pathology. As in the mouse eye, *TSPO* was strongly expressed in both human tissues. Although not as pronounced as in the mouse (Fig. 1A), the significantly lower Ct values indicated stronger expression of *TSPO* in the RPE of the human eye (Fig. 2C). When expression levels in the central and the peripheral retina were blotted separately against donor age (from 17 to 90 years), we observed steady levels of *TSPO* for both the central and peripheral retina and RPE (Fig. 2C) suggesting that *TSPO* expression is not differentially regulated during normal aging. Interestingly however, the peripheral RPE expressed *TSPO* at higher levels than the central RPE (Fig. 2C) whereas expression levels in the central and peripheral retina were not different (data not shown). The implications of this observation are not known and warrant further studies.

Table 3
Real-time PCR primers.

Gene	Forward 5′-3′	Reverse 5′-3′
Actb	CAACGGCTCCGGCATGTGC	CTCTTGCTCTGGGCCTCG
Tspo	GGAACAACCAGCGACTGC	GTACAAAGTAGGCTCCCATGAA
Tnfa	CCACGCTCTTCTGTCTACTGA	GGCCATAGAACTGATGAGAGG
Il6	GCTACCAAACTGGATATAATCAGGA	CCAGGTAGCTATGGTACTCCAGAA
Il1b	ACTACAGGCTCCGAGATGA	CGTTGCTTGGTTCTCCTTG
Gbp6	AGAGAGCAGGACATCAAAGACC	AGCCTCCTTAATTCGATCAGTGT
Arg1	CCTGGCCTTTGTTGATGTC	GGAGTGTTGATGTCAGTGTG
Chil3	TGAGTGGGTTGGTTATGACAAT	CCGTTGAACTTGATCTTATTCTGA
Mrc1	GGTGAACGGAATGATTGTGTA G	CGGTGACCACTCCTGCTG
Cas1	GGCAGGAATTCTGGAGCTTCAA	GTCAGTCCTGGAAATGTGCC
TSPO (human)	TCTGGGGCACGCTCTACT	CAGCAGGAGATCCACCAAGG
ACTB (human)	CCTGGCACCCAGCACAAT	GGGCCGGACTCGTCATAC

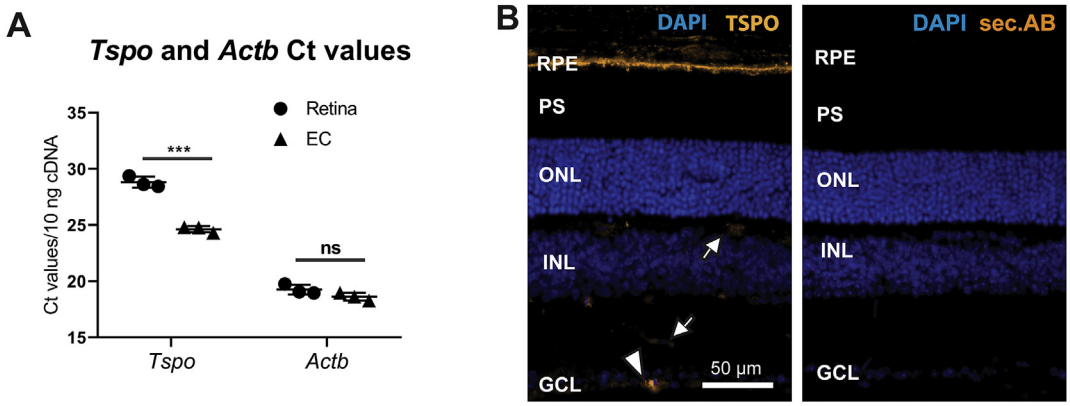

Fig. 1. *Expression of Tspo in the mouse retina and eyecup.* **A)** *Tspo* and *Actb* transcript levels in the retina (circles) and EC (triangles) of wild type mice were determined by real-time PCR in 10 ng of cDNA and shown as Ct values. **B)** Immunofluorescence staining using anti-TSPO antibody (orange, left panel) or secondary antibody only (sec. AB, right panel). Blue: DAPI. Arrows: blood vessels. Arrowhead: positive TSPO signal in the ganglion cell layer (GCL). RPE: retinal pigment epithelium, PS: photoreceptor segments, ONL: outer nuclear layer, INL: inner nuclear layer. N = 3. Statistics: Student t-test. ns: $p > 0.05$, ***: $p \leq 0.001$. Scale bar: 50 µm.

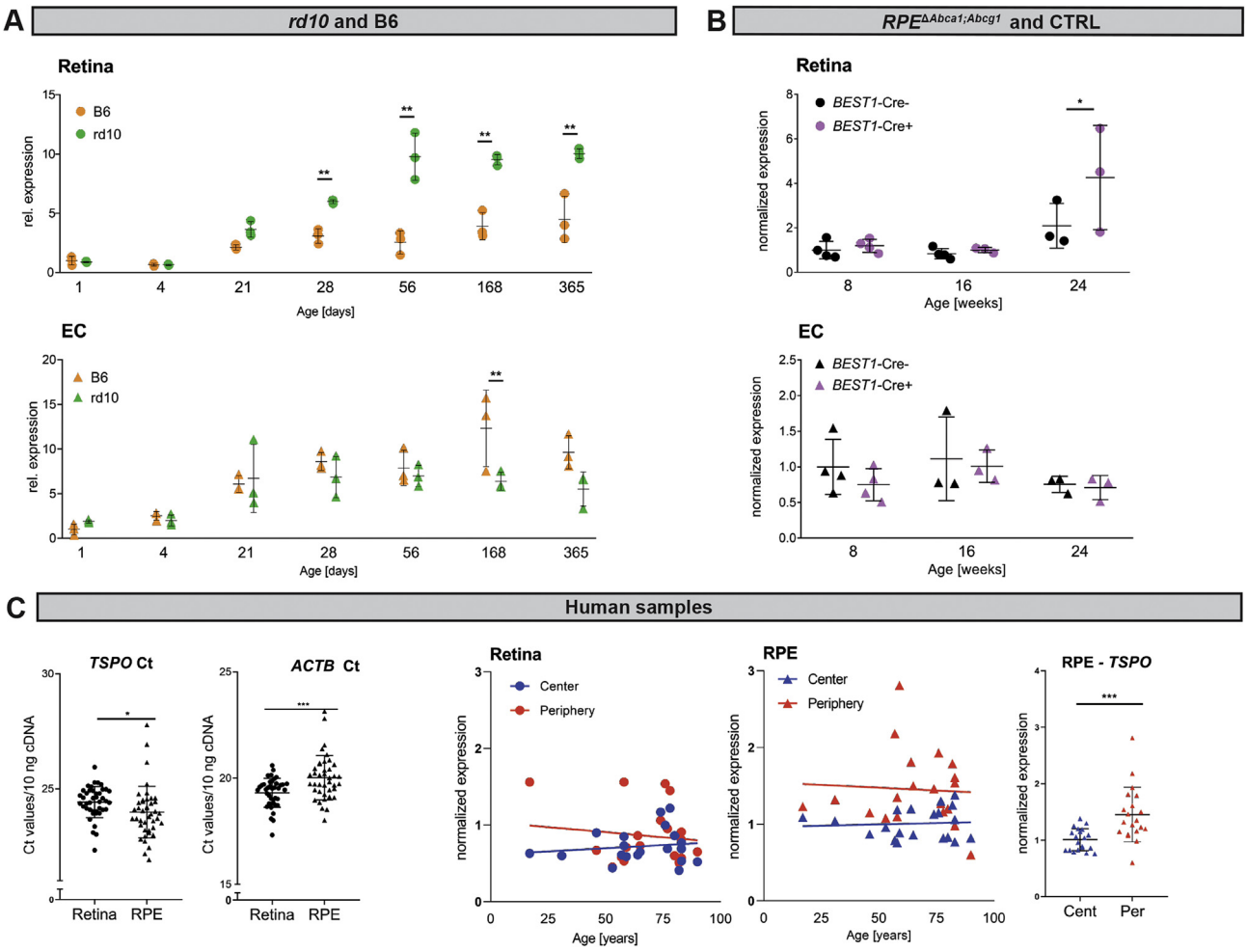

Fig. 2. *Ocular expression of Tspo in mouse models of retinal degeneration and human donor eyes.* **A)** Relative *Tspo* transcript levels in the retina (upper panel) and EC (lower panel) of B6 wild type (B6, orange) and *rd10* (green) mice during post-natal development and ageing. *Tspo* transcript levels are expressed relatively to B6 mice at PND1, which were set to 1 for both retina and EC. **B)** Relative *Tspo* transcript levels in the retina (upper panel) and EC (lower panel) of *RPE*$^{\Delta Abca1;Abcg1}$ (*BEST*- Cre +, magenta) and control (*BEST1*- Cre-, black) mice at 8, 16 and 24 weeks of age. *Tspo* transcript levels are expressed relatively to *BEST1cre*-mice at week 8, which were set to 1 for both retina and EC. N ≥ 3. Shown are individual values and means ± SD. **C)** Left panels: *TSPO* and *ACTB* Ct values were determined in 10 ng of cDNA from central and peripheral retinas and RPE (each dot represents one sample, values for central and peripheral retinas are blotted in the same graph). Shown are individual values and means ± SD. Right panels: relative *TSPO* transcript levels in the central and peripheral retina and RPE of donor eyes expressed as a function of age and comparison of *TSPO* expression levels between central and peripheral human RPE. Cent: central RPE; Per: peripheral RPE. N = 21 donor eyes. Statistics: A, B: *t*-test corrected for multiple comparisons with the Holm-Sidak method; C: Students t-test and linear regression analysis. *$p \leq 0.05$, **$p \leq 0.01$, ***$p \leq 0.001$.

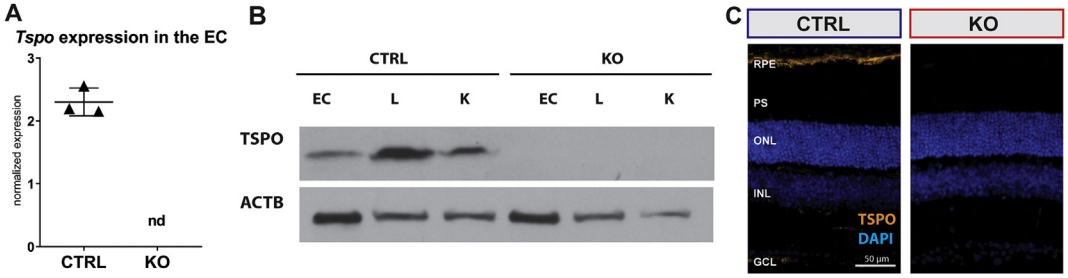

Fig. 3. *Validation of Tspo-KO mice.* **A)** *Tspo* transcript levels in ECs of CTRL and *Tspo-KO* mice were normalized to *Actb* and shown as individual values and means ± SD. nd: not detected. **B)** Detection of TSPO protein levels by Western blotting in EC, liver (L) and kidney (K) lysates of CTRL and *Tspo-KO* mice. ACTB was used as loading control. **C)** Immunofluorescence staining of control (CTRL) and *Tspo-KO* (KO) mice for TSPO (orange). Abbreviations as in Fig. 1. Scale bar: 50 µm. N = 3.

3.3. Validation of the Tspo-KO mouse

To study the consequences of *Tspo* loss in the mouse eye, we generated a full *Tspo-KO* mouse by crossing $Tspo^{flox/flox}$ mice (Sileikyte et al., 2014) with *BEST1*-Cre mice that occasionally activate CRE in the germline (Iacovelli et al., 2011) (see section Material and Methods for more details). The resulting *Tspo-KO* mice lacked the second exon (that contains the AUG start codon) and third exon of the *Tspo* gene. Immunofluorescence staining of retinal cryosections, real-time PCR of cDNA derived from ECs and Western blots of EC, liver and kidney confirmed the absence of TSPO in KO mice (Fig. 3A–C).

3.4. Tspo-KO mice have normal retinal morphology and function

To unveil possible ocular phenotypes arising from the absence of TSPO protein we followed *Tspo-KO* and control (CTRL) mice until 48 weeks of age (Fig. 4). Fundus photography and optical coherence tomography (OCT) at 24 and 48 weeks of age revealed normal fundus appearance and retina layering for both mouse strains (Fig. 4A). Because fundus photography and OCT scans are not suitable to detect minor changes in retinal morphologies, we analysed eyes from CTRL and *Tspo-KO* mice by light microscopy. Analysis confirmed the normal morphology of RPE (Fig. 4B, upper panels) and retina (Fig. 4B, lower panels) in *Tspo-KO* mice at 24 and 48 weeks of age. This is supported by similar numbers of photoreceptor nuclei counted at defined positions along the naso-temporal axis in 24- and 48-week-old CTRL and *Tspo-KO* mice (Fig. 4C).

Because a normal retinal structure may not necessarily translate into normal function, we determined the electroretinographic (ERG) response to light stimuli in CTRL and *Tspo-KO* mice (Fig. 4D and E). Overlays of scotopic (Fig. 4D) and photopic (Fig. 4E) ERG traces recorded from dark- and light-adapted mice, respectively, suggested normal scotopic and photopic retinal function of 48-week-old *Tspo-KO* mice, an interpretation further supported by similar a- and b-wave amplitudes in CTRL and *Tspo-KO* mice at 24 and 48 weeks of age (Fig. 4D and E; right graphs). We therefore concluded that the systemic absence of TSPO did not affect retinal structures or function during development and ageing.

3.5. Tspo-KO and CTRL mice are equally susceptible to retinal degeneration

The fact that TSPO is expressed in activated microglia (reviewed in (Bennett et al., 2016)) and astrocytes (Cosenza-Nashat et al., 2009; Guilarte, 2019) upon neuronal damage and inflammation suggests that TSPO is a stress-related protein. Hence, lack of a phenotype in *Tspo*-KO mice during normal development and ageing may not be surprising. To investigate the consequences of the absence of TSPO for the stressed retina, we induced photoreceptor degeneration by exposing mice to toxic levels of white light. A set of mice kept in darkness served as dark controls (DC). We collected ocular tissues of DCs and light-damaged (LD) mice at 4 and 14 days post-illumination to analyse retinal morphology and count photoreceptor nuclei (Fig. 5A–D). As expected, retinal morphologies of DC mice were intact and normal for both genotypes (Fig. 5B). Following light exposure we observed a time-dependent thinning of the ONL that was similarly extensive in CTRL and *Tspo-KO* mice (Fig. 5C and D). To quantify loss of photoreceptors we counted nuclei in the ONL along the naso-temporal axis (see Material and Methods for more details). The number of photoreceptor nuclei dropped at 4 days post-illumination and was further reduced at 14 days after exposure (Fig. 5A). Importantly, the numbers of photoreceptor nuclei were comparable between CTRL and *Tspo-KO* mice at matching time points suggesting that TSPO did not modulate retinal susceptibility to light-induced photoreceptor degeneration. In addition, lack of TSPO did not influence degeneration in the *rd10* mouse (Fig. 5E and F), even though *Tspo* expression was strongly upregulated during the degeneration phase in *rd10* retinas (Fig. 2). This indicates that TSPO is not essential for disease progression both in induced and inherited models of retinal degeneration.

It is known that light-induced retinal degeneration has an inflammatory component characterized by the transient migration of activated microglia and macrophages into the subretinal space (Joly et al., 2009; Natoli et al., 2016; Ng and Streilein, 2001; Santos et al., 2010; Zhang et al., 2005). Light microscopy of retinal morphologies at 4 days after light exposure suggested the subretinal presence of phagocytic cells both in CTRL and *Tspo-KO* mice (yellow arrowheads in Fig. 5C), indicating that absence of TSPO did not prevent recruitment of such cells to the site of damage.

3.6. Tspo-KO and CTRL mice show comparable mononuclear phagocyte dynamics during light-induced photoreceptor degeneration

TSPO is expressed in activated microglia (reviewed in (Bennett et al., 2016)) and TSPO ligands can modulate microglia activity in brain and retinal pathologies by shifting microglia toward an anti-inflammatory and immunoregulatory state (Scholz et al., 2015). This may lead to a better tissue preservation. However, mechanisms behind ligand-induced modulation of microglia activity and tissue protection are unclear, and data in Fig. 5C suggested that retinal microglia can be activated and/or monocytes recruited also in absence of TSPO. This was confirmed by IBA-1 staining on retinal sections at 4 and 14 days post-illumination (Fig. 6A). Whereas IBA-1 positive cells were found in the inner retina of DC mice, the staining highlighted activated microglia and macrophages in the outer retina of both CTRL and *Tspo-KO* mice at 4 days after light exposure. Some IBA-1 positive cells were still present in the subretinal space of both mice even at 14 days post-exposure. Importantly, we could not identify obvious differences between CTRL and *Tspo-KO* mice with respect to the location of IBA-1 positive immune cells (Fig. 6A). Staining for TSPO confirmed the knockout and demonstrated the presence of TSPO-positive cells in the outer retina of CTRL mice after light exposure (Fig. 6B). These cells were likely the

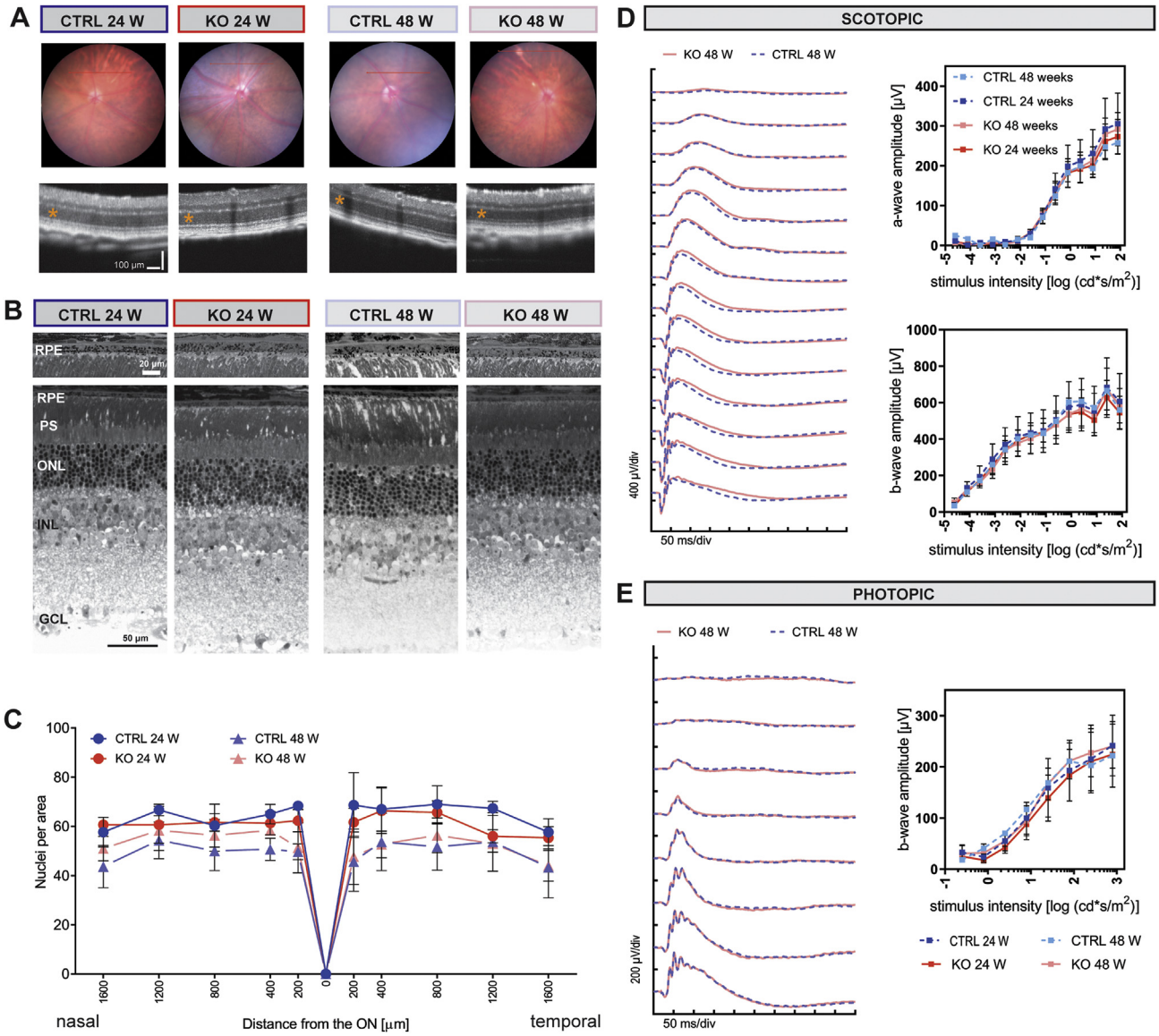

Fig. 4. *Retinal morphology and function in Tspo mice.* **A)** Fundus images (upper panels) and optical coherence tomography (OCT) scans (lower panels) of CTRL and *Tspo-KO* mice at 24 and 48 weeks of age. Asterisks indicate the ONL. **B)** Morphology of RPE (upper panels) and retina (lower panels) of CTRL and *Tspo-KO* mice at 24 and 48 weeks of age. **C)** Number of photoreceptor nuclei per area (see Material and Methods) at the indicated distances from the optic nerve in CTRL (blue lines) and *Tspo-KO* (red lines) mice at 24 (circles) and 48 (triangles) weeks of age. **D)** Scotopic electroretinogram (ERG) recorded from dark-adapted CTRL (dotted blue lines) and *Tspo-KO* (red lines) mice. Left: overlay of averaged traces of mice at 48 weeks of age. Right: a-wave (upper panel) and b-wave (lower panel) amplitudes of CTRL (blue lines) and *Tspo-KO* (red lines) mice at 24 and 48 weeks of age. Amplitudes are blotted against the stimulus intensity. **E)** Photopic ERG recorded from light-adapted CTRL (dotted blue lines) and *Tspo-KO* (red lines) mice. Left: overlay of averaged traces of mice at 48 weeks of age. Right: b-wave amplitudes as a function of stimulus intensity of CTRL (dotted blue lines) and *Tspo-KO* (red lines) mice at 24 and 48 weeks of age. Scale bars: as indicated in the figure. Shown are means ± SD. Statistics: (D, E): two-way ANOVA with Sidak's multiple comparison test. N ≥ 3 (panels A–C). N ≥ 4 (panels D, E). Abbreviations as in Fig. 1.

inflammatory cells detected in Fig. 6A as activated microglia were shown to express TSPO (Karlstetter et al., 2014).

To quantify the number of microglia cells in *Tspo-KO* and control mice, we stained retinal flat mounts with IBA1 (Fig. 6C) and counted cells in the GCL of dark controls and the ONL of light-exposed mice. Data indicate that lack of TSPO did not alter the number of ramified microglia in the GCL of non-exposed mice or the number of activated microglia of an amoeboid shape in the ONL at 4 days after light exposure (Fig. 6D). No microglia were detected in the ONL of dark control mice (not shown).

Because immunofluorescence stainings did not reveal differences in immune cell dynamics following light-exposure we measured expression of pro-inflammatory and anti-inflammatory microglia and macrophage markers (Gong et al., 2019) in whole retina lysates. Pro-inflammatory phagocytes are characterized by the expression of pro-inflammatory cytokines such as tumor necrosis factor-alpha (*Tnfa*) and interleukin-6 (*Il6*) and interleukin-1b (*Il1b*), or interferon-responsive genes, such as guanylate binding protein family member 6 (*Gbp6*) (Gong et al., 2019). The expression of these markers increased similarly in the retina of CTRL and *Tspo-KO* mice after light exposure with *Tnfa, Il6* and *Il1b* showing an early and strong upregulation at 12 h, with *Il1b* slightly increased in *Tspo*-KO mice, followed by a decrease at 4 days (Fig. 6E). *Gbp6* was also increased at 12 h post-illumination and remained elevated at least until 4 days after exposure. Among the anti-inflammatory markers arginase-1 (*Arg1*) was the only gene that did not show an obvious regulation after light-induced damage (Fig. 6F). In contrast, chitinase-like 3 (*Chil3*, also known as *Ym1*) and mannose receptor, C type 1 (*Mrc1*) increased early (*Chil3*) or late (*Mrc1*) after light

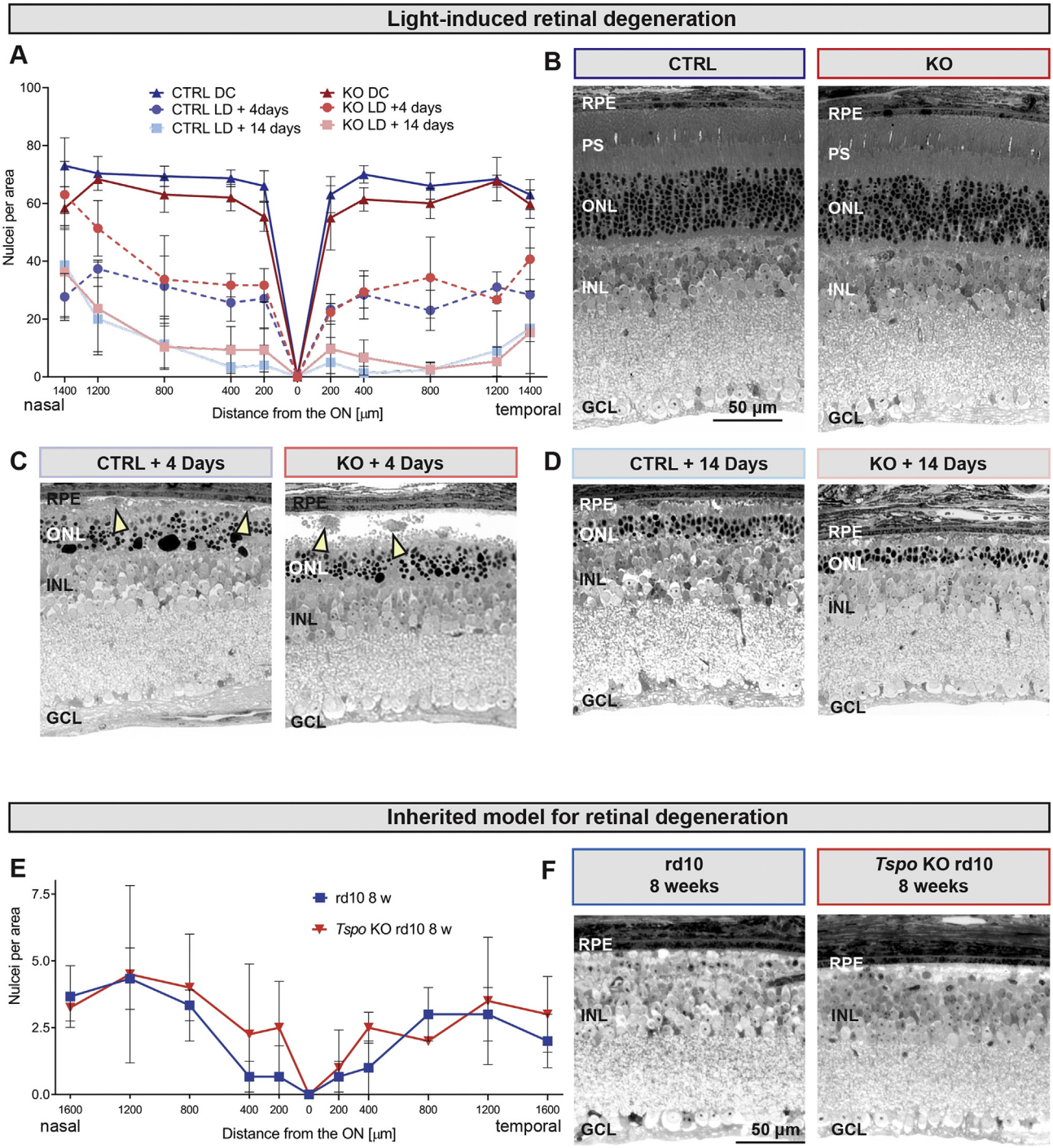

Fig. 5. *Retinal susceptibility to light-induced and inherited degeneration in the absence of Tspo.* **A)** Number of photoreceptor nuclei per area (see Material and Methods) at the indicated distances from the optic nerve head in CTRL (blue lines) and *Tspo-KO* (red lines) mice before (dark control, DC) and at 4 and 14 days after light damage (LD). Shown are means ± SD. **B - D)** Representative morphologies of retinas from CTRL and *Tspo-KO* mice before **(B)**, or at 4 **(C)** and 14 days **(D)** post-illumination. Yellow arrowheads point to phagocytic cells localized in the subretinal space. **E)** Number of photoreceptor nuclei per area at the indicated distances from the optic nerve head in *rd10* (blue lines) and *Tspo-KO;rd10* double mutant (red lines) mice at 8 weeks of age. **F)** Representative morphologies of retinas from *rd10* and *Tspo-KO;rd10* mice at 8 weeks of age. Scale bar: 50 µm. N = 3. Abbreviations as in Fig. 1.

exposure. Similar to the activation and migration of microglia and macrophages, the expression pattern of activation markers after light exposure was comparable for the two mouse strains. We also tested expression levels of Caspase1 (*Casp1*) as this gene was implicated in both apoptotic and inflammatory processes. Expression of *Casp1* was strongly upregulated late in both light-exposed *Tspo-KO* and control mice (Fig. 6G). This suggests that TSPO does not regulate state or activation dynamics of retinal mononuclear phagocytes in our experimental setting.

4. Discussion

After almost four decades of studies, TSPO function remains disputed. It is generally accepted that TSPO is expressed in reactive microglia and astrocytes at the site of brain injury (Anholt et al., 1985) (reviewed in (Rupprecht et al., 2010)) and may thus be relevant for

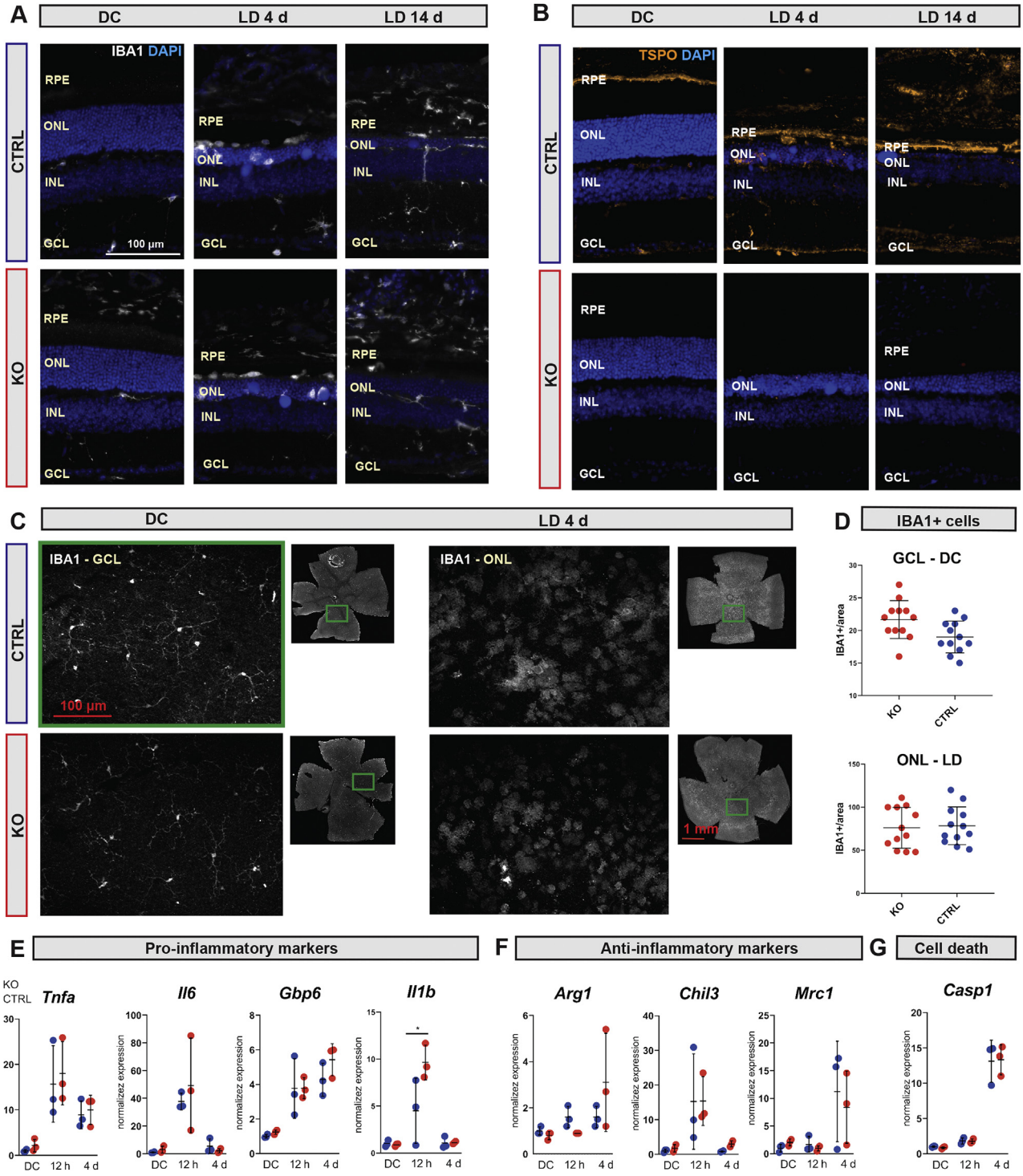

Fig. 6. *Microglia and macrophage dynamics after light-induced degeneration in CTRL and Tspo-KO mice.* **A, B)** Immunofluorescence staining with anti-IBA-1 (white) **(A)** and anti-TSPO (orange) antibodies **(B)** on retinal cryosections of dark controls (DC) and at 4 and 14 days following light damage (LD) as indicated. Blue: DAPI. **C)** Immunofluorescence staining with anti-IBA-1 antibodies (white) of retinal flat mounts prepared from dark controls (DC) or at 4 days after light exposure (LD 4 d). Shown are overview images and images of higher magnifications with the focus plane either on the GCL (DC mice) or the ONL (LD 4 d mice). Note that rectangles in overview images indicate the position of the images with higher magnification but are not to scale **D)** Quantification of IBA1-positive cells in areas of 450 µm^2 × 320 µm^2. Shown are individual values of all 4 areas per retina, as well as means ± SD. Top: microglia in the GCL of DC mice. Bottom: microglia in the ONL of LD mice at 4 d post-exposure. N = 3. **E)** Gene expression levels of the pro-inflammatory microglia and macrophage markers *Tnfa*, *Il6*, *Gbp6* and *Il1b* before and at 12 h and 4 d after light exposure in CTRL (blue) and *Tspo-KO* (red) mice. Shown are individual values and means ± SD of N = 3. **F)** Gene expression levels of the anti-inflammatory microglia and macrophage markers *Arg1*, *Chil3* and *Mrc1* before and at 12 h and 4 d after light exposure in CTRL (blue) and *Tspo-KO* (red) mice. **G)** Gene expression levels of *Casp1* as a marker for apoptotic (cell death) and inflammatory processes. Shown are individual values and means ± SD of N = 3. Scale bars: as indicated.

neural pathologies. Indeed, TSPO ligands showed neuroprotective outcomes in mouse models of neurodegeneration (Girard et al., 2008; Gong et al., 2019; Leva et al., 2017; Scholz et al., 2015) and demonstrated anxiolytic effects in humans (Rupprecht et al., 2010). In addition, more than 40 clinical trials (https://clinicaltrials.gov/ct2/home) tested efficacy of TSPO radioligands for PET imaging of patients suffering from a neurodegenerative disease or traumatic brain injury. To approach TSPO function, it is thus crucial to investigate its expression in neuronal tissues in health and disease.

We showed earlier that TSPO is not only expressed in the retina but also in the RPE of the adult mouse (Scholz et al., 2015; Storti et al., 2019). Here, we established that TSPO has a similar expression profile in human donor eyes, with strong expression of *TSPO* in both retina and RPE. Furthermore, we show that *Tspo* is upregulated in the mouse retina but not in the RPE during retinal degeneration (Fig. 2), independent of whether the degeneration is caused by a mutation affecting primarily the neural retina (*rd10* mice) or the RPE ($RPE^{\Delta Abca1;Abcg1}$ mice). Recent *in vitro* studies of the *TSPO* promoter demonstrated that BV-2 cells (microglia) and ARPE-19 (RPE) cells use different promoter elements for regulating expression providing further evidence for a cell specific and differential regulation of TSPO in immune and RPE cells (Rashid et al., 2018).

The increase of *Tspo* expression in the retina of *rd10* mice coincided with an increase in microglia density in the ONL (Zhao et al., 2015) and elevated expression of inflammatory markers such as interleukin-1beta and caspase-1 (Samardzija et al., 2012). Thus, increased *Tspo* expression in the neural retina likely reflects ongoing inflammatory reactions and microglia activation. Surprisingly however, expression of *Tspo* remained elevated at least until 1 year of age, a time when microglia density in the outer retina has long returned to basal levels (Zhao et al., 2015). During this late phase of degeneration, Müller glia cells may express TSPO as immunofluorescence analysis of 6-month-old *rd10* mice revealed a TSPO staining pattern characteristic for Müller cells in the inner retina (supplementary Figure 1). Müller cell-specific expression of TSPO has already been shown in a mouse model for retinal ischemia (Mages et al., 2019), and a cross-talk between microglia and Müller cells has been suggested during degenerative processes (Roche et al., 2018). Such a cross-talk may include diazepam-binding inhibitor (DBI) that is produced in Müller cells and interacts with TSPO in microglia leading to reduced production of TNFa, lower levels of reactive oxygen species and diminished microglia activity (Wang et al., 2014). The significance of a Müller cell specific expression of TSPO in the degenerated retina (e.g. for gliosis) has still to be determined, especially since absence of TSPO from the *rd10* retina did not influence the degenerative process (Fig. 5E and F).

Like activated microglia, RPE cells are very active phagocytes and participate in the removal of debris from the subretinal space during retinal degeneration. In contrast to microglia, however, RPE cells did not upregulate *Tspo* expression during degenerative processes even when the primary defect was in the RPE ($RPE^{\Delta Abca1;Abcg1}$; *BEST1-Cre* mice, Fig. 2B). Thus, TSPO may not be involved in the phagocytic function of the RPE or activated microglia, a conclusion supported by the absence of an accumulation of cellular debris from the degenerating outer retina in light-damaged and *rd10* mice with or without TSPO (Fig. 5). Taken together our results suggest that *Tspo* expression is regulated in the neural retina but constitutive in the RPE and may not affect phagocytic activities.

In accordance with the idea of TSPO being a stress-related protein, *Tspo-KO* mice did not develop any ocular phenotype and demonstrated normal retinal morphology and function up to 48 weeks of age (Fig. 4). A non-essential function of TSPO for normal mouse physiology is also supported by reports from several groups that independently generated systemic *Tspo-KO* mouse lines (Banati et al., 2014; Barron et al., 2018; Tu et al., 2014; Wang et al., 2016). None of them showed an obvious phenotype, suggesting that TSPO is not necessary for mouse reproduction, development and aging. However, the debate about a potential relevance of TSPO for steroidogenesis has been refuelled by recent studies that reported differential regulation of steroids in adult *Tspo-KO* mice (Barron et al., 2018), as well as in mutant rats and human patients carrying *TSPO* polymorphisms (Owen et al., 2017) (reviewed in (Costa et al., 2018)).

Lack of a retinal phenotype even under stress conditions may also argue against an involvement of TSPO in the mitochondrial permeability transition (MPT) pore, a connection that has been proposed mainly on the basis of effects observed after application of TSPO ligands (Azarashvili et al., 2015). But since such ligands may influence cell physiology also independently of TSPO (Gonzalez-Polo et al., 2005; Hans et al., 2005), a connection of TSPO with MPT is still controversially discussed (Bernardi and Di Lisa, 2015; Chelli et al., 2001; Zoratti et al., 2005). Similarly, the proposed connection of TSPO to mitochondria quality control and regulation of mitophagy (Gatliff et al., 2014, 2017), which also has been implicated in retinal degeneration (Brown et al., 2018; Hyttinen et al., 2018; Lefevere et al., 2017), may not be strengthen by our data since absence of TSPO did not alter progression of degeneration in our models (Fig. 5). The lack of a clearly defined TSPO function and/or phenotype in knockout studies caused several groups to propose the existence of mechanisms that compensate for the absence of TSPO, but the potential nature of such mechanisms has not been identified or discussed in detail (Papadopoulos et al., 2018).

TSPO generates strong interest because of its proven regulation in activated microglia and in astrocytes in the retina and CNS (reviewed in (Bennett et al., 2016)) (Cosenza-Nashat et al., 2009; Guilarte, 2019; Karlstetter et al., 2014; Scholz et al., 2015). Quiescent microglia are ramified and survey the neuronal environment with their processes. In presence of damage they become activated, change their morphology to an amoeboid shape, express TSPO, migrate to the site of damage and initiate phagocytosis of cellular debris. Short-term and controlled microglia activation is beneficial for the damaged tissue. However, long-term unrestrained activation can be detrimental, as microglia might phagocyte also healthy and functional cells (reviewed in (Langmann, 2007)). Thus, a tightly controlled regulation of microglia activity seems pivotal to preserve tissue from further damage. This might be achieved by the application of TSPO ligands that were reported to have microglia-modulatory activity and neuroprotective properties (Gong et al., 2019; Karlstetter et al., 2014; Leva et al., 2017; Scholz et al., 2015). For instance, mice of a model for Parkinson's disease (PD) showed better retention of dopaminergic neurons, improved motor activity and a shift of microglia/macrophages from the pro-inflammatory to the anti-inflammatory state when injected with the TSPO ligand XBD173 (Gong et al., 2019). XBD173 was also shown to modulate the inflammatory behaviour of immune cells in a mouse model for multiple sclerosis (EAE model) leading to improved motor function and preserved myelin basic protein distribution in the CNS (Leva et al., 2017), and to attenuate the response of microglia and Müller cells in a model of retinal ischemia (Mages et al., 2019). Scholz et al. (2015), reported protection against light-induced retinal degeneration by systemic application of XBD173 and attributed the protection to dampened microglia activation. Indeed, *in vitro* assays from the same group showed that XBD173 treatment of murine and human microglia decreased their proliferation and expression of pro-inflammatory cytokines as well as production nitric oxygen radicals (Karlstetter et al., 2014). Similar results were obtained with mouse models for sciatic nerve injury (Girard et al., 2008) where mice treated with etifoxine, another TSPO ligand, exhibited better axonal regeneration, better motor recovery and reduced macrophage infiltration. However, these authors proposed that reduced microglia/macrophage activation might be a bystander effect whereas axonal regrowth was attributed to TSPO-dependent mechanisms intrinsic to neurons themselves. Whether TSPO ligands mediate their protective effects *in vivo* by a direct modulation of microglia activity or by other means is thus still a matter of debate that is further complicated by anxiolytic effects of TSPO ligands (Rupprecht et al., 2009). Such effects

may influence the outcome of tests designed to investigate neuronal function by behavioural assays. We also need to consider that dampened microglia activation observed in several animal models treated with TSPO-ligands could be the consequence of an indirect effect. TSPO-ligands might protect neurons by unknown mechanisms leading to reduced tissue damage and, as a consequence, indirectly to reduced microglia activity.

Considering that various CNS pathologies improved after the application of TSPO ligands (Gong et al., 2019; Leva et al., 2017; Scholz et al., 2015) we expected stronger retinal degeneration and reduced microglia activation in our mouse models when they lacked TSPO. Since this was not the case, we conclude that absence of TSPO does not affect microglia activation or neuronal preservation by itself, but that the interaction of TSPO with a ligand might be fundamental to achieve neuroprotection.

With this work, we demonstrated that *TSPO* is expressed in the neural retina and RPE in mouse and human eyes, but that it is regulated only in the neural retina upon tissue damage. Lack of TSPO did not lead to a retinal phenotype in physiological conditions, did not influence the susceptibility of the retina to degeneration and did not affect microglia and macrophage dynamics in the degenerating retina. We hypothesize that TSPO may not be capable of modulating the course of retinal degeneration by itself but may need interacting partners and/or additional factors to initiate a mechanism that leads to tissue preservation. The identification of these mechanisms may not only help to design neuroprotective strategies but may also shed light onto TSPO function.

Acknowledgements

The authors thank Sarah Nötzli, Cornelia Imsand and Adrian Urwyler for their excellent technical support. This work was supported by grants from VELUX foundation, Switzerland and the Swiss National Science Foundation, Switzerland (31003A_173008).

Appendix A. Supplementary data

Supplementary data to this article can be found online at https://doi.org/10.1016/j.exer.2019.107816.

References

Alexeev, V., Yoon, K., 1998. Stable and inheritable changes in genotype and phenotype of albino melanocytes induced by an RNA-DNA oligonucleotide. Nat. Biotechnol. 16, 1343–1346.
Anholt, R.R., De Souza, E.B., Oster-Granite, M.L., Snyder, S.H., 1985. Peripheral-type benzodiazepine receptors: autoradiographic localization in whole-body sections of neonatal rats. J. Pharmacol. Exp. Ther. 233, 517–526.
Azarashvili, T., Krestinina, O., Baburina, Y., Odinokova, I., Grachev, D., Papadopoulos, V., Akatov, V., Lemasters, J.J., Reiser, G., 2015. Combined effect of G3139 and TSPO ligands on Ca(2+)-induced permeability transition in rat brain mitochondria. Arch. Biochem. Biophys. 587, 70–77.
Banati, R.B., Middleton, R.J., Chan, R., Hatty, C.R., Kam, W.W., Quin, C., Graeber, M.B., Parmar, A., Zahra, D., Callaghan, P., Fok, S., Howell, N.R., Gregoire, M., Szabo, A., Pham, T., Davis, E., Liu, G.J., 2014. Positron emission tomography and functional characterization of a complete PBR/TSPO knockout. Nat. Commun. 5, 5452.
Barron, A.M., Ji, B., Kito, S., Suhara, T., Higuchi, M., 2018. Steroidogenic abnormalities in translocator protein knockout mice and significance in the aging male. Biochem. J. 475, 75–85.
Bennett, M.L., Bennett, F.C., Liddelow, S.A., Ajami, B., Zamanian, J.L., Fernhoff, N.B., Mulinyawe, S.B., Bohlen, C.J., Adil, A., Tucker, A., Weissman, I.L., Chang, E.F., Li, G., Grant, G.A., Hayden Gephart, M.G., Barres, B.A., 2016. New tools for studying microglia in the mouse and human CNS. Proc. Natl. Acad. Sci. U. S. A 113, E1738–E1746.
Bernardi, P., Di Lisa, F., 2015. The mitochondrial permeability transition pore: molecular nature and role as a target in cardioprotection. J. Mol. Cell. Cardiol. 78, 100–106.
Best, L., Ghadery, C., Pavese, N., Tai, Y.F., Strafella, A.P., 2019. New and old TSPO PET radioligands for imaging brain microglial activation in neurodegenerative disease. Curr. Neurol. Neurosci. Rep. 19, 24.
Bitran, D., Foley, M., Audette, D., Leslie, N., Frye, C.A., 2000. Activation of peripheral mitochondrial benzodiazepine receptors in the hippocampus stimulates allopregnanolone synthesis and produces anxiolytic-like effects in the rat. Psychopharmacology 151, 64–71.
Braestrup, C., Albrechtsen, R., Squires, R.F., 1977. High densities of benzodiazepine receptors in human cortical areas. Nature 269, 702–704.
Brown, E.E., Lewin, A.S., Ash, J.D., 2018. Mitochondria: potential targets for protection in age-related macular degeneration. Adv. Exp. Med. Biol. 1074, 11–17.
Caprara, C., Thiersch, M., Lange, C., Joly, S., Samardzija, M., Grimm, C., 2011. HIF1A is essential for the development of the intermediate plexus of the retinal vasculature. Investig. Ophthalmol. Vis. Sci. 52, 2109–2117.
Chang, B., Hawes, N.L., Hurd, R.E., Davisson, M.T., Nusinowitz, S., Heckenlively, J.R., 2002. Retinal degeneration mutants in the mouse. Vis. Res. 42, 517–525.
Chelli, B., Falleni, A., Salvetti, F., Gremigni, V., Lucacchini, A., Martini, C., 2001. Peripheral-type benzodiazepine receptor ligands: mitochondrial permeability transition induction in rat cardiac tissue. Biochem. Pharmacol. 61, 695–705.
Cosenza-Nashat, M., Zhao, M.L., Suh, H.S., Morgan, J., Natividad, R., Morgello, S., Lee, S.C., 2009. Expression of the translocator protein of 18 kDa by microglia, macrophages and astrocytes based on immunohistochemical localization in abnormal human brain. Neuropathol. Appl. Neurobiol. 35, 306–328.
Costa, B., Da Pozzo, E., Martini, C., 2018. Translocator protein and steroidogenesis. Biochem. J. 475, 901–904.
Gatliff, J., East, D., Crosby, J., Abeti, R., Harvey, R., Craigen, W., Parker, P., Campanella, M., 2014. TSPO interacts with VDAC1 and triggers a ROS-mediated inhibition of mitochondrial quality control. Autophagy 10, 2279–2296.
Gatliff, J., East, D.A., Singh, A., Alvarez, M.S., Frison, M., Matic, I., Ferraina, C., Sampson, N., Turkheimer, F., Campanella, M., 2017. A role for TSPO in mitochondrial Ca(2+) homeostasis and redox stress signaling. Cell Death Dis. 8, e2896.
Girard, C., Liu, S., Cadepond, F., Adams, D., Lacroix, C., Verleye, M., Gillardin, J.M., Baulieu, E.E., Schumacher, M., Schweizer-Groyer, G., 2008. Etifoxine improves peripheral nerve regeneration and functional recovery. Proc. Natl. Acad. Sci. U. S. A 105, 20505–20510.
Gong, J., Szego, E.M., Leonov, A., Benito, E., Becker, S., Fischer, A., Zweckstetter, M., Outeiro, T., Schneider, A., 2019. Translocator protein ligand protects against neurodegeneration in the MPTP mouse model of Parkinsonism. J. Neurosci. 39 (19), 3752–3769.
Gonzalez-Polo, R.A., Carvalho, G., Braun, T., Decaudin, D., Fabre, C., Larochette, N., Perfettini, J.L., Djavaheri-Mergny, M., Youlyouz-Marfak, I., Codogno, P., Raphael, M., Feuillard, J., Kroemer, G., 2005. PK11195 potently sensitizes to apoptosis induction independently from the peripheral benzodiazepin receptor. Oncogene 24, 7503–7513.
Grimm, C., Wenzel, A., Stanescu, D., Samardzija, M., Hotop, S., Groszer, M., Naash, M., Gassmann, M., Remé, C., 2004. Constitutive overexpression of human erythropoietin protects the mouse retina against induced but not inherited retinal degeneration. J. Neurosci. 24 (25), 5651–5658.
Guilarte, T.R., 2019. TSPO in diverse CNS pathologies and psychiatric disease: a critical review and a way forward. Pharmacol. Ther. 194, 44–58.
Hans, G., Wislet-Gendebien, S., Lallemend, F., Robe, P., Rogister, B., Belachew, S., Nguyen, L., Malgrange, B., Moonen, G., Rigo, J.M., 2005. Peripheral benzodiazepine receptor (PBR) ligand cytotoxicity unrelated to PBR expression. Biochem. Pharmacol. 69, 819–830.
Hyttinen, J.M.T., Viiri, J., Kaarniranta, K., Blasiak, J., 2018. Mitochondrial quality control in AMD: does mitophagy play a pivotal role? Cell. Mol. Life Sci. : CMLS 75, 2991–3008.
Iacovelli, J., Zhao, C., Wolkow, N., Veldman, P., Gollomp, K., Ojha, P., Lukinova, N., King, A., Feiner, L., Esumi, N., Zack, D.J., Pierce, E.A., Vollrath, D., Dunaief, J.L., 2011. Generation of Cre transgenic mice with postnatal RPE-specific ocular expression. Investig. Ophthalmol. Vis. Sci. 52, 1378–1383.
Jaremko, Ł., Jaremko, M., Giller, K., Becker, S., Zweckstetter, M., 2014. Structure of the Mitochondrial Translocator Protein in Complex with a Diagnostic Ligand. vol. 343. pp. 1363–1366.
Joly, S., Francke, M., Ulbricht, E., Beck, S., Seeliger, M., Hirrlinger, P., Hirrlinger, J., Lang, K.S., Zinkernagel, M., Odermatt, B., Samardzija, M., Reichenbach, A., Grimm, C., Reme, C.E., 2009. Cooperative phagocytes: resident microglia and bone marrow immigrants remove dead photoreceptors in retinal lesions. Am. J. Pathol. 174, 2310–2323.
Karlstetter, M., Nothdurfter, C., Aslanidis, A., Moeller, K., Horn, F., Scholz, R., Neumann, H., Weber, B.H., Rupprecht, R., Langmann, T., 2014. Translocator protein (18 kDa) (TSPO) is expressed in reactive retinal microglia and modulates microglial inflammation and phagocytosis. J. Neuroinflammation 11, 3.
Langmann, T., 2007. Microglia activation in retinal degeneration. J. Leukoc. Biol. 81, 1345–1351.
Lefevere, E., Toft-Kehler, A.K., Vohra, R., Kolko, M., Moons, L., Van Hove, I., 2017. Mitochondrial dysfunction underlying outer retinal diseases. Mitochondrion 36, 66–76.
Leva, G., Klein, C., Benyounes, J., Halle, F., Bihel, F., Collongues, N., De Seze, J., Mensah-Nyagan, A.G., Patte-Mensah, C., 2017. The translocator protein ligand XBD173 improves clinical symptoms and neuropathological markers in the SJL/J mouse model of multiple sclerosis. Biochim. Biophys. Acta (BBA) - Mol. Basis Dis. 1863, 3016–3027.
Liu, G.J., Middleton, R.J., Kam, W.W., Chin, D.Y., Hatty, C.R., Chan, R.H., Banati, R.B., 2017. Functional gains in energy and cell metabolism after TSPO gene insertion. Cell Cycle 16, 436–447.
Mages, K., Grassmann, F., Jagle, H., Rupprecht, R., Weber, B.H.F., Hauck, S.M., Grosche, A., 2019. The agonistic TSPO ligand XBD173 attenuates the glial response thereby protecting inner retinal neurons in a murine model of retinal ischemia. J. Neuroinflammation 16, 43.
Morohaku, K., Pelton, S.H., Daugherty, D.J., Butler, W.R., Deng, W., Selvaraj, V., 2014. Translocator protein/peripheral benzodiazepine receptor is not required for steroid hormone biosynthesis. Endocrinology 155, 89–97.
Natoli, R., Jiao, H., Barnett, N.L., Fernando, N., Valter, K., Provis, J.M., Rutar, M., 2016. A

model of progressive photo-oxidative degeneration and inflammation in the pigmented C57BL/6J mouse retina. Exp. Eye Res. 147, 114–127.
Ng, T.F., Streilein, J.W., 2001. Light-induced migration of retinal microglia into the subretinal space. Investig. Ophthalmol. Vis. Sci. 42, 3301–3310.
Nothdurfter, C., Baghai, T.C., Schule, C., Rupprecht, R., 2012. Translocator protein (18 kDa) (TSPO) as a therapeutic target for anxiety and neurologic disorders. Eur. Arch. Psychiatry Clin. Neurosci. 262 (Suppl. 2), S107–S112.
Owen, D.R., Fan, J., Campioli, E., Venugopal, S., Midzak, A., Daly, E., Harlay, A., Issop, L., Libri, V., Kalogiannopoulou, D., Oliver, E., Gallego-Colon, E., Colasanti, A., Huson, L., Rabiner, E.A., Suppiah, P., Essagian, C., Matthews, P.M., Papadopoulos, V., 2017. TSPO mutations in rats and a human polymorphism impair the rate of steroid synthesis. Biochem. J. 474, 3985–3999.
Papadopoulos, V., Baraldi, M., Guilarte, T.R., Knudsen, T.B., Lacapere, J.J., Lindemann, P., Norenberg, M.D., Nutt, D., Weizman, A., Zhang, M.R., Gavish, M., 2006. Translocator protein (18kDa): new nomenclature for the peripheral-type benzodiazepine receptor based on its structure and molecular function. Trends Pharmacol. Sci. 27, 402–409.
Papadopoulos, V., Fan, J., Zirkin, B., 2018. Translocator protein (18 kDa): an update on its function in steroidogenesis. J. Neuroendocrinol. 30.
Rashid, K., Geissl, L., Wolf, A., Karlstetter, M., Langmann, T., 2018. Transcriptional regulation of Translocator protein (18kDa) (TSPO) in microglia requires Pu.1, Ap1 and Sp factors. Biochimica et biophysica acta. Gene regulatory mechanisms 1861, 1119–1133.
Roche, S.L., Ruiz-Lopez, A.M., Moloney, J.N., Byrne, A.M., Cotter, T.G., 2018. Microglial-induced Muller cell gliosis is attenuated by progesterone in a mouse model of retinitis pigmentosa. Glia 66, 295–310.
Rupprecht, R., Papadopoulos, V., Rammes, G., Baghai, T.C., Fan, J., Akula, N., Groyer, G., Adams, D., Schumacher, M., 2010. Translocator protein (18 kDa) (TSPO) as a therapeutic target for neurological and psychiatric disorders. Nat. Rev. Drug Discov. 9, 971–988.
Rupprecht, R., Rammes, G., Eser, D., Baghai, T.C., Schule, C., Nothdurfter, C., Troxler, T., Gentsch, C., Kalkman, H.O., Chaperon, F., Uzunov, V., McAllister, K.H., Bertaina-Anglade, V., La Rochelle, C.D., Tuerck, D., Floesser, A., Kiese, B., Schumacher, M., Landgraf, R., Holsboer, F., Kucher, K., 2009. Translocator protein (18 kD) as target for anxiolytics without benzodiazepine-like side effects. Science (New York, N.Y.) 325, 490–493.
Samardzija, M., Wariwoda, H., Imsand, C., Huber, P., Heynen, S.R., Gubler, A., Grimm, C., 2012. Activation of survival pathways in the degenerating retina of rd10 mice. Exp. Eye Res. 99, 17–26.
Santos, A.M., Martin-Oliva, D., Ferrer-Martin, R.M., Tassi, M., Calvente, R., Sierra, A., Carrasco, M.C., Marin-Teva, J.L., Navascues, J., Cuadros, M.A., 2010. Microglial response to light-induced photoreceptor degeneration in the mouse retina. J. Comp. Neurol. 518, 477–492.
Schneider, C.A., Rasband, W.S., Eliceiri, K.W., 2012. NIH Image to ImageJ: 25 years of image analysis. Nat. Methods 9, 671–675.
Scholz, R., Caramoy, A., Bhuckory, M.B., Rashid, K., Chen, M., Xu, H., Grimm, C., Langmann, T., 2015. Targeting translocator protein (18 kDa) (TSPO) dampens pro-inflammatory microglia reactivity in the retina and protects from degeneration. J. Neuroinflammation 12, 201.
Selvaraj, V., Stocco, D.M., Tu, L.N., 2015. Minireview: translocator protein (TSPO) and steroidogenesis: a reappraisal. Molecular endocrinology (Baltimore, Md 29, 490–501.
Sileikyte, J., Blachly-Dyson, E., Sewell, R., Carpi, A., Menabo, R., Di Lisa, F., Ricchelli, F., Bernardi, P., Forte, M., 2014. Regulation of the mitochondrial permeability transition pore by the outer membrane does not involve the peripheral benzodiazepine receptor (Translocator Protein of 18 kDa (TSPO)). J. Biol. Chem. 289, 13769–13781.
Storti, F., Klee, K., Todorova, V., Steiner, R., Othman, A., van der Velde-Visser, S., Samardzija, M., Meneau, I., Barben, M., Karademir, D., Pauzuolyte, V., Boye, S.L., Blaser, F., Ullmer, C., Dunaief, J.L., Hornemann, T., Rohrer, L., den Hollander, A., von Eckardstein, A., Fingerle, J., Maugeais, C., Grimm, C., 2019. Impaired ABCA1/ABCG1-mediated lipid efflux in the mouse retinal pigment epithelium (RPE) leads to retinal degeneration. eLife 8.
Storti, F., Raphael, G., Griesser, V., Klee, K., Drawnel, F., Willburger, C., Scholz, R., Langmann, T., von Eckardstein, A., Fingerle, J., Grimm, C., Maugeais, C., 2017. Regulated efflux of photoreceptor outer segment-derived cholesterol by human RPE cells. Exp. Eye Res. 165, 65–77.
Tu, L.N., Morohaku, K., Manna, P.R., Pelton, S.H., Butler, W.R., Stocco, D.M., Selvaraj, V., 2014. Peripheral benzodiazepine receptor/translocator protein global knock-out mice are viable with no effects on steroid hormone biosynthesis. J. Biol. Chem. 289, 27444–27454.
Tu, L.N., Zhao, A.H., Hussein, M., Stocco, D.M., Selvaraj, V., 2016. Translocator protein (TSPO) affects mitochondrial fatty acid oxidation in steroidogenic cells. Endocrinology 157, 1110–1121.
Wang, H., Zhai, K., Xue, Y., Yang, J., Yang, Q., Fu, Y., Hu, Y., Liu, F., Wang, W., Cui, L., Chen, H., Zhang, J., He, W., 2016. Global deletion of TSPO does not affect the viability and gene expression profile. PLoS One 11, e0167307.
Wang, M., Wang, X., Zhao, L., Ma, W., Rodriguez, I.R., Fariss, R.N., Wong, W.T., 2014. Macroglia-microglia interactions via TSPO signaling regulates microglial activation in the mouse retina. J. Neurosci. : Off. J.Soc. Neurosci. 34, 3793–3806.
Wenzel, A., Reme, C.E., Williams, T.P., Hafezi, F., Grimm, C., 2001. The Rpe65 Leu450Met variation increases retinal resistance against light-induced degeneration by slowing rhodopsin regeneration. J. Neurosci. : Off. J.Soc. Neurosci. 21, 53–58.
Zhang, C., Shen, J.K., Lam, T.T., Zeng, H.Y., Chiang, S.K., Yang, F., Tso, M.O., 2005. Activation of microglia and chemokines in light-induced retinal degeneration. Mol. Vis. 11, 887–895.
Zhao, L., Zabel, M.K., Wang, X., Ma, W., Shah, P., Fariss, R.N., Qian, H., Parkhurst, C.N., Gan, W.B., Wong, W.T., 2015. Microglial phagocytosis of living photoreceptors contributes to inherited retinal degeneration. EMBO Mol. Med. 7, 1179–1197.
Zoratti, M., Szabo, I., De Marchi, U., 2005. Mitochondrial permeability transitions: how many doors to the house? Biochim. Biophys. Acta 1706, 40–52.